

Reconstruction of stochastic nonlinear dynamical models from trajectory measurements

V. N. Smelyanskiy^{1,*}, D. G. Luchinsky^{1,2}, D. A. Timuçin¹, and A. Bandrivskyy²

¹*NASA Ames Research Center, Mail Stop 269-2, Moffett Field, CA 94035, USA and*

²*Department of Physics, Lancaster University, Lancaster LA1 4YB, UK*

A new algorithm is presented for reconstructing stochastic nonlinear dynamical models from noisy time-series data. The approach is analytical; consequently, the resulting algorithm does *not* require an extensive global search for the model parameters, provides optimal compensation for the effects of dynamical noise, and is robust for a broad range of dynamical models. The strengths of the algorithm are illustrated by inferring the parameters of the stochastic Lorenz system and comparing the results with those of earlier research. The efficiency and accuracy of the algorithm are further demonstrated by inferring a model for a system of five globally- and locally-coupled noisy oscillators.

PACS numbers: 02.50.Tt, 05.45.Tp, 05.10.Gg, 87.19.Hh, 05.45.Pq

Keywords: Dynamical inference, nonlinear time-series analysis, chaotic dynamics

I. INTRODUCTION

Stochastic nonlinear dynamical models are widely used in studying complex (natural as well as man-made) phenomena; examples range from molecular motors [1] and semiconductor lasers [2] to epidemiology [3] and coupled matter–radiation systems in astrophysics [4]. Accordingly, much attention has been paid in the statistical physics community to the central problem of reconstructing (i.e., inferring) stochastic nonlinear dynamical models from noisy measurements (see, e.g., [5, 6]). The chief difficulty here stems from the fact that, in a great number of important problems, it is not possible to derive a suitable model from “first principles,” and one is therefore faced with a rather broad range of possible parametric models to consider. Furthermore, experimental data can sometimes be extremely skewed due to the intricate interplay between noise and nonlinearity, making it very difficult to extract from data important “hidden” features (e.g., coupling parameters) of a model.

Although no general method exists for inferring the parameters of stochastic nonlinear dynamical models from measurements, various schemes have been proposed recently [7, 8, 9, 10, 11, 12, 13, 14, 15] to deal with different aspects of this “inversion” problem. An important numerical technique, suggested in [12, 13, 14], is based on estimating drift and diffusion coefficients at a number of points in the phase space of the dynamical system. This technique was extended further in [15] to handle both dynamical and measurement noise. In principle, this approach allows subsequent use of the least-squares method for the estimation of the model parameters. Such an empirical approach, however, requires a considerable amount of data and an intensive computational effort even for a simple stochastic equation. A more general, and efficient, theoretical approach is therefore very desir-

able.

Arguably the most general approach to the solution of this problem is furnished by Bayes’ theorem [8, 10, 16]. Indeed, it was shown in [9] that the Bayesian method provides a rigorous and systematic basis for heuristic modifications made earlier [7] to the least-squares method to enable its use on noisy measurements. The Bayesian approach was employed in [8] to estimate levels of dynamical and measurement noise for a known dynamical model. The Bayesian method has also been used for parameter estimation in maps in the presence of dynamical [9] and weak measurement [10] noise. Finally, an application of the Bayesian method to continuous systems was considered in [11].

A common drawback of these earlier works is their exclusive reliance on numerical methods for the optimization of cost functions and the evaluation of multi-dimensional normalization integrals encountered in the theory. This disadvantage becomes increasingly more pronounced when systems with ever larger numbers of unknown parameters are investigated. Another major deficiency is that most of the earlier works deal with discrete maps, and the corresponding results are therefore not immediately applicable to continuous systems, since the transformation from noise variables to dynamical variables is different in discrete and continuous cases. Specifically, as will be shown below, a prefactor accounting for the Jacobian of the transformation must be included in the likelihood function in the continuous case. Such a prefactor was considered in [11] in the context of Bayesian inference for continuous systems; however, an *ad hoc* likelihood function was used there instead of the correct form derived here.

In this paper, we introduce a new technique for Bayesian inference of stochastic nonlinear dynamical models from noisy measurements. At the core of our algorithm is a path-integral representation of the likelihood function that yields the correct form for the Jacobian prefactor. This term provides optimal compensation for the effects of dynamical noise, thus leading to robust inference for a broad range of dynamical models. Another

*Electronic address: Vadim.N.Smelyanskiy@nasa.gov

key feature of the approach is a novel parameterization of the vector “force” field, which permits an analytical treatment of the inference problem, thus obviating the need for extensive global optimization. These improvements lead to an efficient and accurate algorithm for reconstructing from time-series data models of stochastic nonlinear dynamical systems with large numbers of unknown parameters.

The paper is organized as follows. The general formulation of the problem and its analytical solution are presented in Section II. The algorithm is then applied in Section III A to data from the stochastic Lorenz system, and its performance is compared with those of earlier research. The advantages of the present method are further illustrated in Section III B by inferring a model for a system of five globally- and locally-coupled noisy oscillators. Finally, the results are discussed and conclusions are drawn in Section IV.

II. THEORY OF RECONSTRUCTION OF STOCHASTIC NONLINEAR DYNAMICAL MODELS

A. Problem description

We envision a typical experimental situation where the stochastic trajectory $\mathbf{x}(t)$ of a dynamical system is measured at sequential time instants $\{t_n; n = 0, 1, \dots, N\}$, and a set of data $\mathcal{Y} = \{\mathbf{y}_n \equiv \mathbf{y}(t_n)\}$ is thus obtained. For instance, $\mathbf{x}(t)$ may represent the coordinates of a molecular motor progressing along a microtubule [1] or the fluctuating Stokes vector of a semiconductor laser field [2]. Our objective is to extract from \mathcal{Y} all available information regarding the dynamical evolution of $\mathbf{x}(t)$. As mentioned in Section I, we advocate the Bayesian approach for the solution of this problem. Toward this end, one has to introduce a parametric model for the dynamical system and a statistical model for the measurements. These elements allow one to incorporate into the solution of the reconstruction problem any available *a priori* information on the time-series data (stationarity, embedding dimension, etc.), as well as expert domain knowledge (e.g., a theoretical analysis of the physics problem at hand).

The dynamical and measurement equations commonly adopted in the context of model reconstruction are

$$\left. \begin{aligned} \dot{\mathbf{x}}(t) &= \mathbf{f}(\mathbf{x}; \mathbf{c}) + \boldsymbol{\xi}(t), \\ \mathbf{y}(t) &= \mathbf{x}(t) + \boldsymbol{\nu}(t), \end{aligned} \right\} \quad (1)$$

with $\mathbf{x}, \mathbf{y}, \boldsymbol{\xi}, \boldsymbol{\nu} \in \mathbb{R}^L$, and $\mathbf{f} : \mathbb{R}^L \mapsto \mathbb{R}^L$. Here, the first equation represents the dynamical model in the form of a set of coupled nonlinear Langevin equations with a vector field $\mathbf{f}(\mathbf{x}; \mathbf{c})$ parameterized by unknown coefficients $\mathbf{c} \in \mathbb{R}^M$, and the second equation relates the observations to the system trajectory. We assume that the additive dynamical and measurement noise processes $\boldsymbol{\xi}(t)$

and $\boldsymbol{\nu}(t)$ are stationary, white, and Gaussian with

$$\left. \begin{aligned} \langle \boldsymbol{\xi}(t) \rangle &= \mathbf{0}, & \langle \boldsymbol{\xi}(t) \boldsymbol{\xi}^T(t') \rangle &= \hat{\mathbf{D}} \delta(t - t'), \\ \langle \boldsymbol{\nu}(t) \rangle &= \mathbf{0}, & \langle \boldsymbol{\nu}(t) \boldsymbol{\nu}^T(t') \rangle &= \epsilon^2 \hat{\mathbf{I}} \delta(t - t'), \end{aligned} \right\} \quad (2)$$

where $\hat{\mathbf{D}}$ and ϵ are also typically unknown. Thus, the elements $\{c_m; m = 1, 2, \dots, M\}$ of the model coefficient vector \mathbf{c} , the elements $\{D_{ll'}; l, l' = 1, 2, \dots, L\}$ of the dynamical noise covariance (or diffusion) matrix $\hat{\mathbf{D}}$, and the measurement noise intensity ϵ^2 together constitute the complete set

$$\mathcal{M} = \{\mathbf{c}, \hat{\mathbf{D}}, \epsilon\} \quad (3)$$

of unknown parameters. The model reconstruction problem, then, is that of inferring the elements of the parameter set \mathcal{M} from the measured time-series data \mathcal{Y} .

B. Bayesian inference

In Bayesian model inference, two distinct probability density functions (PDFs) are ascribed to the set of unknown model parameters: the *prior* $p_{\text{pr}}(\mathcal{M})$ and the *posterior* $p_{\text{ps}}(\mathcal{M}|\mathcal{Y})$, respectively representing our state of knowledge about \mathcal{M} before and after processing a block of data \mathcal{Y} . These two PDFs are related to each other via Bayes’ theorem [5]:

$$p_{\text{ps}}(\mathcal{M}|\mathcal{Y}) = \frac{p(\mathcal{Y}|\mathcal{M}) p_{\text{pr}}(\mathcal{M})}{\int p(\mathcal{Y}|\mathcal{M}) p_{\text{pr}}(\mathcal{M}) d\mathcal{M}}. \quad (4)$$

Here, the *sampling distribution* $p(\mathcal{Y}|\mathcal{M})$ is the conditional PDF of the measurements \mathcal{Y} for a given choice of the model \mathcal{M} ; it is also referred to, as we do, as the *likelihood* of \mathcal{M} given \mathcal{Y} . Meanwhile, the prior acts as a *regularizer*, concentrating the parameter search to those regions of the model space favored by our expertise and any available auxiliary information. This initial assignment of probabilities must, of course, be “coherent” [17], i.e., consistent, at least implicitly, with the physics of the problem. In practice, (4) can be applied iteratively using a sequence of data blocks $\mathcal{Y}, \mathcal{Y}', \dots$; the posterior computed from block \mathcal{Y} serves as the prior for the next block \mathcal{Y}' , etc. For a sufficiently large number of observations, $p_{\text{ps}}(\mathcal{M}|\mathcal{Y}, \mathcal{Y}', \dots)$ becomes sharply peaked around a most probable model \mathcal{M}^* .

We note that Bayes theorem allow for a simple geometric interpretation and has a clear physical sense. Indeed, denote by \mathcal{M} all the events corresponding every possible values of the model parameters (these events are encircled in the figure 1 by the solid line). The events corresponding to the measured time-series data are shown by \mathcal{X} . Then the intersection of the two sets of events can be factories in two ways $P(\mathcal{X} \cap \mathcal{M}) = P(\mathcal{X}|\mathcal{M})P(\mathcal{M}) = P(\mathcal{M}|\mathcal{X})P(\mathcal{X})$, where $P(\mathcal{X}|\mathcal{M})$ and $P(\mathcal{M}|\mathcal{X})$ are corresponding conditional probabilities. Taking into account that $P(\mathcal{X}) = \int d\mathcal{M} P(\mathcal{X}|\mathcal{M})P(\mathcal{M})$ and dividing last equation by $P(\mathcal{X})$

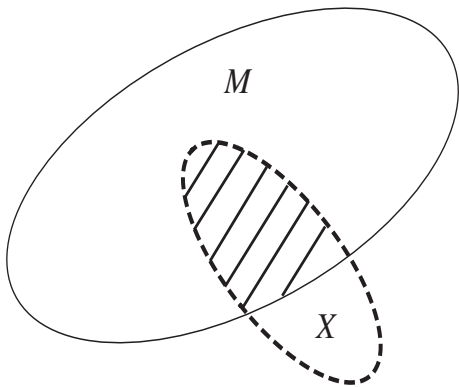


FIG. 1: Illustration of the geometrical interpretation and physical meaning the Bayes theorem. \mathcal{M} denotes set of all possible values of the model parameters. Events corresponding to the measured time-series data are shown by \mathcal{X} . Intersection of the two sets is shown by the shaded area. The geometrical interpretation of the Bayes theorem is that the likelihood function cuts out of the all possible model parameters those that correspond to the observed time-series data.

we have Bayes theorem. then geometrical interpretation of the Bayes theorem is that the likelihood function cuts out of the all possible model parameters those that correspond to the observed time-series data. It has a clear physical meaning that states that given initial guess about model parameters it can be improved using results of the measurements. This theorem plays fundamental role in the modern theory of measurements.

The main thrust of recent research on stochastic nonlinear dynamical model reconstruction [7, 9, 10, 11] has been directed towards developing (i) efficient optimization algorithms for extracting the most probable model \mathcal{M}^* from the posterior, and (ii) efficient multi-dimensional integration techniques for evaluating the normalization factor in the denominator of (4). These efforts have mostly employed *ad hoc* expressions for the likelihood function (see, e.g., the cost function of Eq. (31) in [11]); consequently, the resulting inference schemes fail to properly compensate for the effects of noise. In fact, it appears that there is a lack in the model-reconstruction literature of a closed-form expression (expanded to correct orders in the sampling period) for the likelihood function of the measurements of a continuous system trajectory.

Below we introduce a new approach to Bayesian inference of stochastic nonlinear dynamical models. The method has two key analytical features. Firstly, the likelihood function is written in the form of a path integral over the stochastic system trajectory, which includes a prefactor that optimally compensates for the detrimental effects of (dynamical) noise. Secondly, we suggest a novel parameterization of the unknown vector field, which renders the inference problem essentially linear for a broad class of nonlinear dynamical systems, and thus helps us find optimal parameter estimates without extensive numerical optimization. These features enable

us to write an efficient and accurate Bayesian inference algorithm for reconstructing models of nonlinear dynamical systems driven by noise. As a prelude to the formal development that follows, the reader may at this point wish to review the theory given in Appendix A for the maximum-likelihood reconstruction of a one-dimensional system model.

C. The likelihood function

As we pointed out above, one of the central challenges in the inference of stochastic nonlinear dynamical models is the derivation of a suitable likelihood function that optimally compensates for the effects of noise. A key ingredient in this context is the probability density functional $\mathcal{F}_{\mathcal{M}}[\mathbf{x}(t)]$ of finding the system in “state” $\mathbf{x}(t)$ at time t [11, 18, 19, 20]. This is supplemented by $p_{\text{ob}}(\mathcal{Y}|\mathcal{X})$ denoting the PDF of observing a time series \mathcal{Y} for a specific realization $\mathcal{X} = \{\mathbf{x}_n\}$ of the system trajectory. Thus, we may express the likelihood function very generally in the form of a path integral over the random trajectories of the dynamical system as

$$p(\mathcal{Y}|\mathcal{M}) = \int_{\mathbf{x}(t_i)}^{\mathbf{x}(t_f)} p_{\text{ob}}(\mathcal{Y}|\mathcal{X}) \mathcal{F}_{\mathcal{M}}[\mathbf{x}(t)] \mathcal{D}\mathbf{x}(t), \quad (5)$$

giving the probabilistic relationship between the observations \mathcal{Y} and the unknown parameters \mathcal{M} of the model (1). Here, we choose $t_i \ll t_0 < t_N \leq t_f$ so that $p(\mathcal{Y}|\mathcal{M})$ does not depend on the particular initial and final states $\mathbf{x}(t_i)$, $\mathbf{x}(t_f)$. We note that the path-integral approach has also proved useful in nonlinear filtering of random signals (see, e.g., [24]) where standard spectral and correlation analyses fail.

The explicit form of $\mathcal{F}_{\mathcal{M}}[\mathbf{x}(t)]$ has been given in [21, 22, 23]; however, in the context of dynamical inference, it is not necessary to employ this exact form as one can usually rely on the smallness of the sampling interval. Accordingly, adopting a uniform sampling scheme $t_n = t_0 + nh$, we assume here for the sake of simplicity that $h \equiv (t_N - t_0)/N$ is small, and rewrite (1) using a mid-point Euler discretization scheme in the form

$$\left. \begin{aligned} \mathbf{x}_{n+1} &= \mathbf{x}_n + h \mathbf{f}(\tilde{\mathbf{x}}_n; \mathbf{c}) + \mathbf{z}_n, \\ \mathbf{y}_n &= \mathbf{x}_n + \boldsymbol{\nu}_n, \end{aligned} \right\} \quad (6)$$

where $\tilde{\mathbf{x}}_n \equiv \frac{1}{2}(\mathbf{x}_{n+1} + \mathbf{x}_n)$, while \mathbf{z}_n are independent, zero-mean, Gaussian random variables with covariance $\langle \mathbf{z}_n \mathbf{z}_{n'}^T \rangle = h \hat{\mathbf{D}} \delta_{nn'}$. The probability of a particular realization $\{\mathbf{z}_n\}$ of the dynamical noise process is simply

$$\mathcal{P}[\{\mathbf{z}_n\}] = \prod_{n=0}^{N-1} \frac{d\mathbf{z}_n}{\sqrt{(2\pi h)^L |\hat{\mathbf{D}}|}} \exp\left(-\frac{1}{2h} \mathbf{z}_n^T \hat{\mathbf{D}}^{-1} \mathbf{z}_n\right). \quad (7)$$

Changing to dynamical state variables using (6), we thus obtain the desired PDF for the dynamical system (1) to have an arbitrary trajectory $\{\mathbf{x}_n\}$:

$$\begin{aligned} \mathcal{F}_{\mathcal{M}}[\{\mathbf{x}_n\}] &= p_{\text{st}}(\mathbf{x}_0) J(\{\mathbf{x}_n\}) \\ &\times \prod_{n=0}^{N-1} \frac{1}{\sqrt{(2\pi h)^L |\hat{\mathbf{D}}|}} \exp\left(-\frac{1}{2h} [\mathbf{x}_{n+1} - \mathbf{x}_n - h \mathbf{f}(\tilde{\mathbf{x}}_n; \mathbf{c})]^T \hat{\mathbf{D}}^{-1} [\mathbf{x}_{n+1} - \mathbf{x}_n - h \mathbf{f}(\tilde{\mathbf{x}}_n; \mathbf{c})]\right), \end{aligned} \quad (8)$$

where $p_{\text{st}}(\mathbf{x})$ signifies the stationary distribution of $\mathbf{x}(t)$, and the Jacobian of the transformation is given by

$$\begin{aligned} J(\{\mathbf{x}_n\}) &= \left| \left\{ \frac{\partial z_{ln}}{\partial x_{l'n'}} \right\} \right| \simeq \prod_{n=1}^N \prod_{l=1}^L \left[1 - \frac{h}{2} \frac{\partial f_l(\tilde{\mathbf{x}}_n; \mathbf{c})}{\partial x_{ln}} \right] \\ &\simeq \exp\left[-\frac{h}{2} \sum_{n=1}^N \text{tr} \hat{\Phi}(\tilde{\mathbf{x}}_n; \mathbf{c})\right], \end{aligned} \quad (9)$$

approximated to leading order in h , with the elements of the matrix $\hat{\Phi}$ defined as $\Phi_{ll'}(\mathbf{x}; \mathbf{c}) \equiv \partial f_l(\mathbf{x}; \mathbf{c}) / \partial x_{l'}$.

The evaluation of (5) requires, in addition, that we adopt a specific form for the measurement PDF

$p_{\text{ob}}(\mathcal{Y}|\mathcal{X})$. We assume here that, for each trajectory component $x_l(t)$, the measurement error ϵ is negligible compared with the fluctuations induced by the dynamical noise; i.e., $\epsilon^2 \ll hD_{ll}$. Consequently, we may use

$$p_{\text{ob}}(\mathcal{Y}|\mathcal{X}) \simeq \prod_{n=0}^N \delta(\mathbf{y}_n - \mathbf{x}_n) \quad (10)$$

in (5), and the set of unknown model parameters to be inferred from data reduces to $\mathcal{M} = \{\mathbf{c}, \hat{\mathbf{D}}\}$. With this substitution, (5) is easily evaluated; introducing $\tilde{\mathbf{y}}_n \equiv \frac{1}{2}(\mathbf{y}_{n+1} + \mathbf{y}_n)$, we write the result in the form

$$\begin{aligned} -\frac{2}{N} \ln p(\mathcal{Y}|\mathcal{M}) &= -\frac{2}{N} p_{\text{st}}(\mathbf{y}_0) + L \ln(2\pi h) + \ln |\hat{\mathbf{D}}| \\ &+ \frac{h}{N} \sum_{n=0}^{N-1} \left\{ \text{tr} \hat{\Phi}(\tilde{\mathbf{y}}_n; \mathbf{c}) + [\dot{\mathbf{y}}_n - \mathbf{f}(\tilde{\mathbf{y}}_n; \mathbf{c})]^T \hat{\mathbf{D}}^{-1} [\dot{\mathbf{y}}_n - \mathbf{f}(\tilde{\mathbf{y}}_n; \mathbf{c})] \right\}, \end{aligned} \quad (11)$$

where we introduced the “velocity” $\dot{\mathbf{y}}_n \equiv (\mathbf{y}_{n+1} - \mathbf{y}_n)/h$. It is important to note that this likelihood function is asymptotically exact in the limit $h \rightarrow 0$ and $N \rightarrow \infty$, with the total observation duration $T = Nh$ remaining constant.

It is the term $\text{tr} \hat{\Phi}(\tilde{\mathbf{y}}_n; \mathbf{c})$ in the above that provides optimal compensation for the detrimental effects of dynamical noise, and distinguishes our likelihood function from those introduced in earlier works. Formally, this term emerges from the path integral as the Jacobian of the transformation from noise variables to dynamical variables [22, 25]. We emphasize, however, that this is *not* merely a correction term, but is in fact crucial for accurate inference. In particular, for a small attractor (with characteristic length scale smaller than square root of the noise intensity) the inference is only possible due to this term as will be shown in Section III.

D. Parameterization of the unknown vector field

As mentioned in Section I, one of the main difficulties encountered in the inference of stochastic nonlinear dynamical models is that the cost function, defined in (15) below, is generally nonlinear in the model parameters,

thus requiring the use of extensive numerical optimization methods for finding its global minimum. The parameterization we now introduce avoids this difficulty while still encompassing a broad class of nonlinear dynamical models. Indeed, many of the model reconstruction examples considered in earlier works on stochastic nonlinear dynamical inference can be solved within this framework. Moreover, a large number of important practical applications (see, e.g., [26, 27]) can also be treated using the same approach.

We parameterize the nonlinear vector field in the form

$$\mathbf{f}(\mathbf{x}; \mathbf{c}) = \hat{\mathbf{U}}(\mathbf{x}) \mathbf{c}, \quad (12)$$

where $\hat{\mathbf{U}}(\mathbf{x})$ is an $L \times M$ matrix of suitably chosen basis functions, and \mathbf{c} is an M -dimensional vector of unknown parameters. The choice of basis functions is open to any appropriate class of (polynomial, trigonometric, etc.) functions that may be required for a satisfactory representation of the vector field. In general, if we use G different basis functions $\{\phi_g(\mathbf{x}); g = 1, 2, \dots, G\}$ to model the vector field \mathbf{f} , then the matrix $\hat{\mathbf{U}}$ will have the block structure

$$\hat{\mathbf{U}} = \left[\begin{array}{c} \left(\begin{array}{cccc} \phi_1 & 0 & \dots & 0 \\ 0 & \phi_1 & \dots & 0 \\ \vdots & \vdots & \ddots & \vdots \\ 0 & 0 & \dots & \phi_1 \end{array} \right) \left(\begin{array}{cccc} \phi_2 & 0 & \dots & 0 \\ 0 & \phi_2 & \dots & 0 \\ \vdots & \vdots & \ddots & \vdots \\ 0 & 0 & \dots & \phi_2 \end{array} \right) \dots \left(\begin{array}{cccc} \phi_G & 0 & \dots & 0 \\ 0 & \phi_G & \dots & 0 \\ \vdots & \vdots & \ddots & \vdots \\ 0 & 0 & \dots & \phi_G \end{array} \right) \end{array} \right], \quad (13)$$

comprising G diagonal blocks of size $L \times L$ ($M = GL$), with the \mathbf{x} dependence suppressed for brevity. An important feature of (12) for our subsequent development is that, while possibly highly nonlinear in \mathbf{x} , $\mathbf{f}(\mathbf{x}; \mathbf{c})$ is strictly linear in \mathbf{c} .

As shown next, (11) and (12) are the two main ingredients that enable an analytic solution to the problem of stochastic nonlinear dynamical model inference from time-series data.

E. The algorithm

We start by choosing a prior model PDF that is Gaussian in \mathbf{c} and uniform in $\hat{\mathbf{D}}$:

$$p_{\text{pr}}(\mathcal{M}) \propto \exp \left[-\frac{1}{2}(\mathbf{c} - \mathbf{c}_{\text{pr}})^T \hat{\Sigma}_{\text{pr}} (\mathbf{c} - \mathbf{c}_{\text{pr}}) \right]. \quad (14)$$

Substituting (12), (14), and the likelihood $p(\mathcal{Y}|\mathcal{M})$ given by (11) into (4), we obtain the posterior model PDF in the form $p_{\text{ps}}(\mathcal{M}|\mathcal{Y}) = \text{const} \times \exp[-S_{\mathcal{Y}}(\mathbf{c}, \hat{\mathbf{D}})]$, where

$$S_{\mathcal{Y}}(\mathbf{c}, \hat{\mathbf{D}}) = \rho_{\mathcal{Y}}(\hat{\mathbf{D}}) - \mathbf{c}^T \mathbf{w}_{\mathcal{Y}}(\hat{\mathbf{D}}) + \frac{1}{2} \mathbf{c}^T \hat{\Sigma}_{\mathcal{Y}}(\hat{\mathbf{D}}) \mathbf{c} \quad (15)$$

is the cost function whose global minimum yields the most probable model $\mathcal{M}^* = \{\mathbf{c}^*, \hat{\mathbf{D}}^*\}$. Here, use was made of the definitions

$$\rho_{\mathcal{Y}}(\hat{\mathbf{D}}) = \frac{h}{2} \sum_{n=0}^{N-1} \dot{\mathbf{y}}_n^T \hat{\mathbf{D}}^{-1} \dot{\mathbf{y}}_n + \frac{N}{2} \ln |\hat{\mathbf{D}}|, \quad (16)$$

$$\mathbf{w}_{\mathcal{Y}}(\hat{\mathbf{D}}) = \hat{\Sigma}_{\text{pr}} \mathbf{c}_{\text{pr}} + h \sum_{n=0}^{N-1} \left[\hat{\mathbf{U}}_n^T \hat{\mathbf{D}}^{-1} \dot{\mathbf{y}}_n - \frac{1}{2} \mathbf{v}_n \right], \quad (17)$$

$$\hat{\Sigma}_{\mathcal{Y}}(\hat{\mathbf{D}}) = \hat{\Sigma}_{\text{pr}} + h \sum_{n=0}^{N-1} \hat{\mathbf{U}}_n^T \hat{\mathbf{D}}^{-1} \hat{\mathbf{U}}_n, \quad (18)$$

where $\hat{\mathbf{U}}_n \equiv \hat{\mathbf{U}}(\tilde{\mathbf{y}}_n)$, $\mathbf{v}_n \equiv \mathbf{v}(\tilde{\mathbf{y}}_n)$, and the components of the vector $\mathbf{v}(\mathbf{x})$ are

$$v_m(\mathbf{x}) = \sum_{l=1}^L \frac{\partial U_{lm}(\mathbf{x})}{\partial x_l}, \quad m = 1, 2, \dots, M. \quad (19)$$

For a given block of data \mathcal{Y} of length $(N+1)$, the best estimates for the model parameters are given by the posterior means of \mathbf{c} and $\hat{\mathbf{D}}$, which coincide with the global minimum of $S_{\mathcal{Y}}(\mathbf{c}, \hat{\mathbf{D}})$. We handle this optimization problem in the following way. Assume for the moment that

\mathbf{c} is known in (15); for the first iteration, take $\mathbf{c} = \mathbf{c}_{\text{pr}}$. Then, minimizing $S_{\mathcal{Y}}(\mathbf{c}, \hat{\mathbf{D}})$ with respect to $\hat{\mathbf{D}}$, we find that the posterior distribution over $\hat{\mathbf{D}}$ has a mean

$$\langle \hat{\mathbf{D}} \rangle = \frac{1}{N} \sum_{n=0}^{N-1} (\dot{\mathbf{y}}_n - \hat{\mathbf{U}}_n \mathbf{c}) (\dot{\mathbf{y}}_n - \hat{\mathbf{U}}_n \mathbf{c})^T. \quad (20)$$

Assume next that $\hat{\mathbf{D}}$ is known, and note from (15) that in this case, the posterior distribution over \mathbf{c} is Gaussian. Its covariance is given by $\hat{\Sigma}_{\mathcal{Y}}(\hat{\mathbf{D}})$, and its mean

$$\langle \mathbf{c} \rangle = \hat{\Sigma}_{\mathcal{Y}}^{-1}(\hat{\mathbf{D}}) \mathbf{w}_{\mathcal{Y}}(\hat{\mathbf{D}}) \quad (21)$$

minimizes $S_{\mathcal{Y}}(\mathbf{c}, \hat{\mathbf{D}})$ with respect to \mathbf{c} . Thus, for the second iteration, \mathbf{c}_{pr} and $\hat{\Sigma}_{\text{pr}}$ are replaced with $\langle \mathbf{c} \rangle$ and $\hat{\Sigma}_{\mathcal{Y}}(\hat{\mathbf{D}})$, respectively. This two-step (analytical) optimization procedure is continued iteratively until convergence, which is typically much faster than brute-force numerical optimization that has been attempted in earlier works.

It is worthwhile to pause here and reflect on the content of (17). The first term in the sum is essentially the generalized least-squares (GLS) result (see Appendix B), and vanishes at the attractors of the dynamical system (1). On the other hand, the second term in the sum on the right-hand side of (17), originating from the term $\text{tr} \hat{\Phi}(\tilde{\mathbf{y}}_n; \mathbf{c})$ in (11), does not vanish at an attractor, and is in fact crucial for accurate inference in the presence of noise. This can be demonstrated analytically by rewriting the sum in integral form as

$$\begin{aligned} \mathbf{w}_{\mathcal{Y}}(\hat{\mathbf{D}}) &= \hat{\Sigma}_{\text{pr}} \mathbf{c}_{\text{pr}} + \int_{\mathbf{x}(t_0)}^{\mathbf{x}(t_0+T)} \hat{\mathbf{U}}[\mathbf{y}(t)]^T \hat{\mathbf{D}}^{-1} d\mathbf{y} \\ &\quad - \frac{1}{2} \int_{t_0}^{t_0+T} \mathbf{v}[\mathbf{y}(t)] dt. \end{aligned} \quad (22)$$

It can now be seen that, for an attractor localized in the phase space, the first integral will remain finite since the initial and final points of integration both belong to the attractor. Meanwhile, the second integral in (22) will grow with the duration of observation T . In particular, for a point attractor, the first integral is identically zero and the second, ‘‘compensating’’ term alone contributes to inference. This result is intuitively clear since, in the absence of noise, the system will stay forever at the same point (i.e., the point attractor) and no structure can be inferred. It is the dynamical noise that forces the system

to move about in the phase space, thus making it possible to infer its structure from time-series data.

In general, then, both of the integral terms in (22) are needed to optimally compensate for the effects of dynamical noise and thus enable robust convergence of our inference algorithm. The relative importance of these two terms will be investigated quantitatively in the following section.

III. INFERENCE EXAMPLES

We have verified the accuracy and robustness of our algorithm on several different types of dynamical systems. Here, we discuss its performance on two representative examples.

A. The Lorenz system

We start with the archetypical chaotic nonlinear system of Lorenz,

$$\left. \begin{aligned} \dot{x}_1 &= \sigma(x_2 - x_1) + \xi_1(t), \\ \dot{x}_2 &= r x_1 - x_2 - x_1 x_3 + \xi_2(t), \\ \dot{x}_3 &= x_1 x_2 - b x_3 + \xi_3(t), \end{aligned} \right\} \quad (23)$$

augmented by zero-mean Gaussian noise processes $\xi_l(t)$ with covariance $\langle \xi_l(t) \xi_{l'}(t') \rangle = D_{ll'} \delta(t - t')$. Synthetic data (with no measurement noise) were generated by simulating (23) using the standard parameter set $\sigma = 10$, $r = 28$, $b = \frac{8}{3}$, and for various levels of dynamical noise intensities as explained below. The phase portrait of the Lorenz system with dynamical noise is shown in Figure 2 along with the noiseless case to visually convey the difficulty of the inference problem.

1. Parameter estimation with strong dynamical noise

We compare now the performance of our algorithm with the results of earlier work [11]. No attempt was made in [11] to identify the model of the system and only four unknown parameters were estimated.

In parameter estimation, the functional form of the nonlinear force field – in this case, the right-hand side of (23) – is assumed known, and the associated coefficients are then estimated from data. This is the approach reported in [11], where the diffusion matrix is taken in the form $\hat{\mathbf{D}} = \tau^2 \hat{\mathbf{I}}$, and the unknown parameters $\{\sigma, r, b, \tau^2\}$ are estimated via extensive numerical optimization of a cost function by simulated annealing and back-propagation techniques. We now demonstrate that our algorithm can estimate the parameters of the system (23) extremely efficiently and with very high accuracy.

First we notice that since the diffusion matrix is diagonal, our algorithm is reduced in this case to the trivial

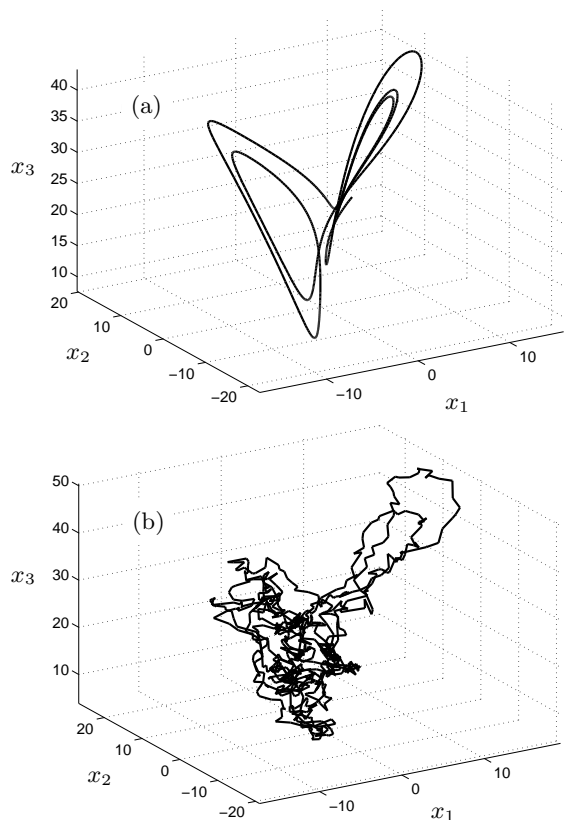


FIG. 2: The phase portrait of the chaotic nonlinear Lorenz system (23) with the standard parameters (see text): (a) deterministic system; (b) stochastic system with strong dynamical noise, simulated with a diagonal diffusion matrix having elements $D_{11} = 1500$, $D_{22} = 1600$, and $D_{33} = 1700$. (All quantities in the equations and figures are dimensionless in this paper.)

one-dimensional analytical solution of the problem for each equation in the form (cf with (17), (18), (20), (21) and see Appendix A for the details)

$$\mathbf{c}_i = \hat{\mathbf{H}}_i^{-1} \mathbf{w}_i, \quad i = 1 \dots 3$$

where

$$w_{il} = \sum_{n=0}^{N-1} \left(c_{il} \phi_{il} - \frac{\tau^2}{2} \frac{\partial \phi_{il}}{\partial x_i} \right)$$

and

$$\hat{\mathbf{H}}_i = \sum_{n=0}^{N-1} \begin{pmatrix} \phi_{i1} \phi_{i1} & \phi_{i1} \phi_{i2} & \dots & \phi_{i1} \phi_{iL} \\ \phi_{i2} \phi_{i1} & \phi_{i2} \phi_{i2} & \dots & \phi_{i2} \phi_{iL} \\ \vdots & \vdots & \ddots & \vdots \\ \phi_{iL} \phi_{i1} & \phi_{iL} \phi_{i2} & \dots & \phi_{iL} \phi_{iL} \end{pmatrix}.$$

Noise intensity is found according to (20). We note that in each equation we now have different basis functions ϕ_{il} . For the first equation we have the following two

basis functions: $\phi_{11} = x_1$ and $\phi_{12} = x_2$. For the second equation we have: $\phi_{21} = x_1$, $\phi_{22} = x_2$, and $\phi_{23} = x_1 x_3$. And for the last equation we have: $\phi_{31} = x_1 x_2$, $\phi_{32} = x_3$.

Thus there are a total of 8 unknown parameters to be estimated: a seven-dimensional coefficient vector \mathbf{c} and the noise intensity τ^2 . (Note that this is already more ambitious than what was done in [11], since we are attempting to estimate *all* model coefficients, including those that are equal to ± 1 .)

The convergence of our scheme is so rapid that it is feasible to use the algorithm in real time on “streaming” data. To make a fair comparison we use the same number of data points as in [11]. As an indication of the inference accuracy, we quote in Table I results for data simulated with the standard Lorenz parameter set and two values of dynamical noise intensity for weak and strong cases.

Now we turn to an extension of our approach that allows for efficient identification of the Lorenz system from a substantially extended model space with 33 unknown parameters.

2. Model reconstruction with strong dynamical noise

When the analytical form of the nonlinear force field is not known *a priori*, one may adopt a parametric model, as was done in (12); in this setting, it is more appropriate to refer to the inference problem as model reconstruction. In practical terms, the main difference between parameter estimation and model reconstruction is in the number of unknown parameters involved, which is typically an order of magnitude larger in the latter case. This proliferation of unknowns is one of the main reasons why inference methods that rely on brute-force numerical techniques are rendered largely impracticable for model reconstruction. On the other hand, owing to its analytical foundation, our algorithm is quite capable of handling this more difficult task, as we demonstrate below.

TABLE I: Inference results for the parameters of the system (23) with weak (first set) and strong (second set) dynamical noise. A synthetic data set of 4,000 points was generated for each case by simulating the system with a diffusion matrix $\hat{\mathbf{D}} = \tau^2 \hat{\mathbf{I}}$, and subsequently sampling its trajectory with $h = 0.002$.

<i>Parameter</i>	<i>Value</i>	<i>Estimate</i>
σ	10.00	9.9916
r	28.00	27.8675
b	2.667	2.6983
τ	1.00	0.9965
σ	10.00	9.9039
r	28.00	28.3004
b	2.667	2.8410
τ	40.00	39.9108

TABLE II: Inference results for the parameters of the model (24). (For brevity, only a representative subset of the $b_{ll''}$ and $D_{ll''}$ parameters is shown.) Synthetic data, comprising 200 blocks of 600,000 points each, were generated by simulating the system with the standard Lorenz parameter set and a diagonal diffusion matrix, and subsequently sampling its trajectory with $h = 0.005$.

<i>Parameter</i>	<i>Value</i>	<i>Estimate</i>
a_{11}	-10.00	-10.55
a_{21}	28.00	27.53
a_{31}	0.0	-0.43
a_{12}	10.00	10.77
a_{22}	-1.00	-0.194
a_{32}	0.0	0.596
a_{13}	0.0	0.065
a_{23}	0.0	0.001
a_{33}	-2.667	-2.759
b_{111}	0.0	0.013
b_{211}	0.0	0.001
b_{311}	0.0	0.018
b_{112}	0.0	0.002
b_{212}	0.0	-0.012
b_{312}	1.00	0.995
b_{113}	0.0	-0.016
b_{213}	-1.00	-0.985
D_{11}	1500.0	1522.1
D_{22}	1600.0	1621.5
D_{33}	1700.0	1713.4

We start by considering the data set of Figure 2, where the structure of the Lorenz attractor is drastically obscured by the presence of strong dynamical noise (almost 2 orders of magnitude stronger than in [11]). We wish to fit this data set with a polynomial model of quadratic nonlinearity. Toward this end, we introduce a parametric model of the form

$$\dot{x}_l = \sum_{l'=1}^3 a_{ll'} x_{l'}(t) + \sum_{l',l''=1}^3 b_{ll'l''} x_{l'}(t) x_{l''}(t) + \xi_l(t), \quad (24)$$

$l, l', l'' = 1, 2, 3$. Including the elements of the (symmetric) diffusion matrix $\hat{\mathbf{D}}$, we now have a total of 33 unknown parameters comprising the set $\mathcal{M} = \{a_{ll'}, \{b_{ll'l''}\}, \{D_{ll''}\}\}$. Despite the restriction to linear, bilinear, and quadratic polynomial basis functions, (24) still represents an extremely broad class of dynamical models. Assuming no measurement noise for simplicity, the application of our algorithm entails the use of equations (20) and (21) with (17) and (18). The inferred parameter values are shown in Table II; it can be seen that, even in this case of extremely strong dynamical noise, our algorithm succeeds in accurately reconstructing the Lorenz model.

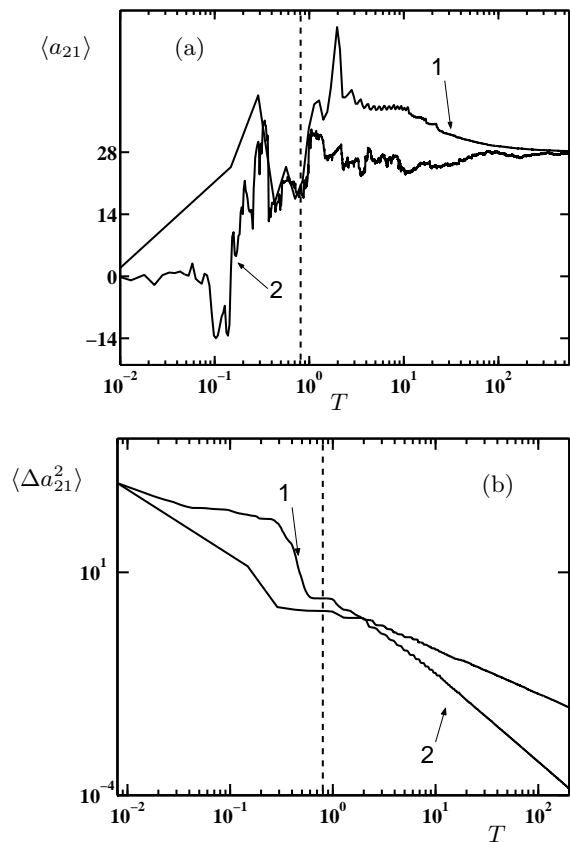


FIG. 3: Results for (a) the posterior mean (i.e., inferred value) and (b) the posterior variance (i.e., associated uncertainty) of the model parameter a_{21} corresponding to parameter r of the Lorenz system (24) as a function of increasing observation duration. Curve 1: $\{D_{ll}\} = \{0.01, 0.012, 0.014\}$, $h = 0.002$; curve 2: $\{D_{ll}\} = \{100, 120, 140\}$, $h = 0.00002$. The time instant of step-like decrease in the variance is indicated by the vertical dashed line.

3. Accuracy of the inferred parameters

The accuracy of the reconstruction depends on a number of factors. As an example, consider the inferred values and variances of the Lorenz parameter r as a function of the total observation duration, shown in Figure 3 for two different levels of noise. Of particular note is a sharp, step-like decrease in the variances that occurs on the same time scale as the period of system oscillations, $\tau_{\text{osc}} \simeq 0.6$ (marked by the dashed line in Figure 3). In addition to the total observation duration T , the inference error is also sensitive to the values of the sampling interval h and the noise intensities D_{ll} . For example, for the parameters of curve 1 in Figure 3, the relative inference error was 0.015%. When the noise intensity was increased by a factor of 10^4 (curve 2 in Figure 3), the ratio T/h (i.e., the number of data points N) had to be increased by at least a factor of 250 to achieve an inference error below 1%.

TABLE III: Inference results for the parameters of the model (24), obtained using 200 blocks of 600,000 data points each, sampled at $h = 0.005$. True and inferred parameter values are shown along with the corresponding error (relative and absolute errors for the nonzero and zero parameters, respectively). The inference error is below 1% for all parameters, and much less for most.

Parameter	Value	Estimate	% error
a_{11}	-10.0000	-9.9984	0.0161
a_{21}	28.0000	28.0139	0.0496
a_{31}	0.0	-0.0052	-0.5180
a_{21}	10.0000	9.9982	0.0178
a_{22}	-1.0000	-1.0051	0.5120
a_{23}	0.0	0.0031	0.3072
a_{31}	0.0	0.0014	0.1390
a_{32}	0.0	0.0015	0.1542
a_{33}	-2.6667	-2.6661	0.0196
b_{111}	0.0	0.0002	0.0179
b_{211}	0.0	0.0002	0.0238
b_{311}	0.0	-0.0004	-0.0401
b_{112}	0.0	-0.0002	-0.0208
b_{212}	0.0	-0.0002	-0.0223
b_{312}	1.0000	1.0006	0.0607
b_{113}	0.0	-0.0001	-0.0111
b_{213}	-1.0000	-1.0004	0.0446
D_{11}	0.2867	0.2865	0.0587
D_{22}	0.4087	0.4081	0.1564
D_{33}	0.5118	0.5148	0.5946
$D_{12} = D_{21}$	0.2052	0.2049	0.1442
$D_{13} = D_{31}$	0.1069	0.1061	0.7657
$D_{23} = D_{32}$	0.1814	0.1812	0.1028

We have observed that it is generally possible to achieve arbitrarily accurate inference results with a (sufficiently small) fixed sampling interval by increasing the total duration of observation; this is true even in the case of a full (i.e., non-diagonal) diffusion matrix. Indeed, we were able to achieve highly accurate parameter estimates for sampling intervals ranging from 10^{-6} to 0.01 and noise intensities ranging from 0 to 10^2 . As an example, we summarize in Table III our inference results for the model (24) with a full diffusion matrix, showing extremely high accuracy.

4. Optimal compensation for the noise-induced errors

Finally, we would like to demonstrate the importance of the Jacobian prefactor (9) included in our likelihood function by examining the inference results obtained with and without this term. As shown in Figure 4 for parameter r of the Lorenz system, the omission of the prefactor in the likelihood function results in a systematic underestimation of this parameter, whereas the inclusion of this term leads to an accurate inference as it optimally compensates for the effects of dynamical noise.

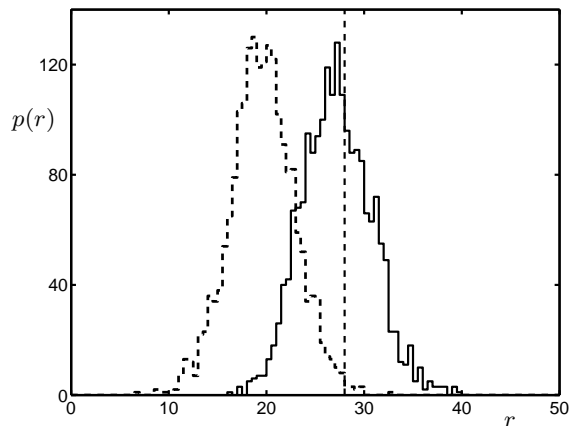


FIG. 4: Demonstration of improved inference accuracy due to the prefactor (9) in the likelihood function. The true value of the parameter being inferred is indicated by the vertical dashed line. The solid and dashed curves respectively show the histograms of parameter values inferred by our algorithm and by the generalized least-squares method, which lacks the Jacobian prefactor. The histograms were built from an ensemble of 1,000 numerical experiments with 90,000 data points each.

5. Discussion of results

The Lorenz system provides a concrete example with which to emphasize the advantages of our algorithm over previous work. We note firstly that we derive the correct form of the likelihood function and avoid using of *ad hoc* likelihood function introduced in [11]. Furthermore, we obtain analytical solution of the problem. This innovations allow us to estimate model parameters of the Lorenz system much faster and more accurately using the same number of points as in [11]. Furthermore, our results unlike the results reported in [11] do not depend neither on the choice of initial values for the model parameters nor on the *ad hoc* conditions imposed on the analysis of the experimental data to exclude points from certain regions of the phase space.

The computational efficiency of our algorithm also allows us to lift the practical limitation on the total number of data points used for inference in previous work. (The relatively small number of points (4,000) used for inference in [11] was dictated by the complexity of the extensive numerical optimization algorithms used therein.) In our approach to inference, processing of $\mathcal{O}(10^5)$ data points takes only a few seconds on a personal computer with a 1-GHz CPU, therefore enabling the use of very large data sets to achieve arbitrarily accurate model reconstruction.

More importantly, the efficiency of our algorithm allows us to extend substantially the dimensionality of the model space. As a consequence it can be efficiently applied to deal with a more general problem of model reconstruction, when the functional form of a nonlinear vector

field is unknown

B. A system of five coupled oscillators

The limitations of inference algorithms that rely on numerical methods for global optimization and multi-dimensional integration come into sharper focus when systems with large numbers of model parameters are investigated. We now wish to illustrate the advantages of our algorithm by inferring a model for a system comprising five locally- and globally-coupled van der Pol oscillators with $\mathcal{O}(10^2)$ unknown model parameters.

With $K = 5$, the system under study is

$$\left. \begin{aligned} \dot{u}_k &= v_k, \\ \dot{v}_k &= \varepsilon_l (1 - u_k^2) v_k - \omega_l u_k + \sum_{k'=1 \setminus k}^K \eta_{kk'} u_{k'} \\ &+ u_k [\gamma_{k(k-1)} u_{k-1} + \gamma_{k(k+1)} u_{k+1}] \\ &+ \sum_{k'=1}^K \sigma_{kk'} \mu_{k'}, \end{aligned} \right\} \quad (25)$$

where $\{\mu_k(t)\}$ are mutually independent, zero-mean, unit-variance, delta-correlated, Gaussian noise processes. We assume (for simplicity) that there is no measurement noise, and that the state is partially observed to produce the signal $\mathbf{y} = [v_1 \ v_2 \ v_3 \ v_4 \ v_5]^T$. The state of the system is thus described by the 10-dimensional vector $\mathbf{x} = [u_1 \ \dots \ u_5 \ v_1 \ \dots \ v_5]^T$. We note, however, that values of u_k in the model (25) are assumed to be known and do not have to be inferred. Therefore the problem is reduced to the inference of the model parameters of five couple equations for v_k , which are parameterized according to the (12) with $\mathbf{D} = \sigma\sigma^T$.

The phase portrait of this system, projected onto the (u_1, u_2, u_3) subspace of its phase space, is shown in Figure 5 for some nominal set of model parameters.

We choose the following basis functions with which to reconstruct the model:

$$\begin{aligned} \phi_k &= u_k, \\ \phi_{k+K} &= v_k, \\ \phi_{k+2K} &= u_k^2 v_k, \\ \phi_{1+3K} &= u_1^2, \\ \phi_{2+3K} &= u_1 u_2, \\ &\vdots \\ \phi_{15+3K} &= u_5^2, \end{aligned}$$

$k = 1, 2, \dots, K$. Together with the elements of the (symmetric) diffusion matrix $\hat{\mathbf{D}}$, we thus have a total of 165 model parameters to infer. We summarize in Table IV the results of our algorithm for the first oscillator, once again showing high inference accuracy. Additionally, the convergence of the parameters of the fifth oscillator and the noise intensities to their correct values is shown in Figure 6 as a function of the amount of data used.

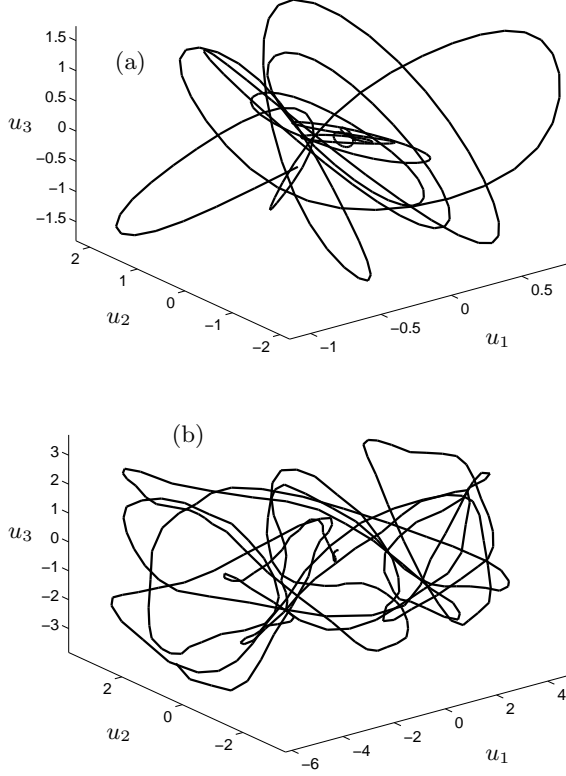


FIG. 5: The phase portrait of the system (25) as projected onto the (u_1, u_2, u_3) subspace: (a) deterministic system; (b) stochastic system with a diagonal diffusion matrix of the form $\hat{\mathbf{D}} = 100\hat{\mathbf{I}}$. (Note the scale change between the axes of the two figures.) See Table IV and Figure 6 for the values of some of the model parameters used in the simulation.

In order to further highlight the vital noise compensation effect provided by the prefactor term in the likelihood function used in the present work, we compare in Figure 7 inference results for one of the coefficients of the system (25), ε_1 , obtained with two different diffusion matrices $\hat{\mathbf{D}}$ and $\hat{\mathbf{D}}/4$, where the matrix $\hat{\mathbf{D}}$ chosen at random to be

$$\hat{\mathbf{D}} = \begin{bmatrix} 3.9628 & 2.9636 & 0.6176 & 2.4941 & 2.5068 \\ 2.9636 & 5.5045 & 2.7690 & 5.2893 & 5.5421 \\ 0.6176 & 2.7690 & 4.6974 & 4.8813 & 3.0284 \\ 2.4941 & 5.2893 & 4.8813 & 7.1428 & 4.6732 \\ 2.5068 & 5.5421 & 3.0284 & 4.6732 & 7.5784 \end{bmatrix}. \quad (26)$$

As discussed earlier, without the Jacobian prefactor (9), (21) reduces to the GLS estimator. Figure 7 shows that the GLS estimator systematically overestimates the value of ε_1 ; the larger the noise intensity, the larger the systematic error, reaching a few hundred per cent in this case, as shown by curves 1' and 2'. On the other hand, when the proper Jacobian prefactor is included in the likelihood function as in (11), we are able to achieve optimal compensation of the noise-induced errors, as shown by

TABLE IV: Inference results for the parameters of the first oscillator in the system (25), obtained using 50 blocks of 150,000 data points each, sampled at $h = 0.06$. The inference error is well below 1% for all parameters.

Parameter	Value	Estimate	% error
ε_1	-8.40	-8.4167	0.2
ω_1	-4.4000	-4.4031	0.07
η_{12}	0.4400	0.4432	0.7
η_{13}	-0.60	-0.6033	0.54
η_{14}	0.96	0.9625	0.3
η_{15}	0.80	0.8022	0.3
γ_{12}	-0.480	-0.4806	0.1
γ_{15}	0.8	0.8013	0.2
Q_{11}	0.20	0.2020	1.0

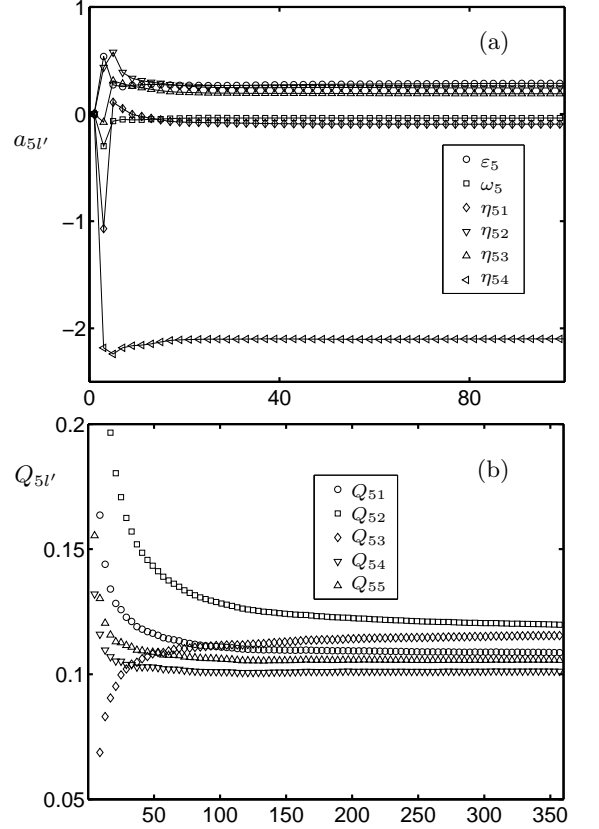


FIG. 6: Accurate inference of (a) the parameters of the fifth oscillator in the system (25) and (b) the elements of the last row of the diffusion matrix \mathbf{Q} . The horizontal axes show the number of blocks of data used, with 800 points in each block, sampled at $h = 0.02$.

curves 1 and 2 obtained with the same noise intensities.

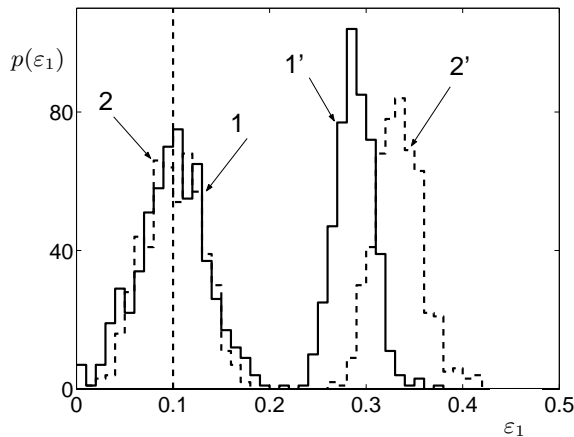


FIG. 7: Further demonstration of improved inference accuracy due to the prefactor (9) in the likelihood function. The true value of the parameter being inferred is indicated by the vertical dashed line. Histograms 1 and 2 show results obtained with our algorithm, while histograms 1' and 2' are due to the GLS method, showing the detrimental effect on inference accuracy of the missing prefactor. The diffusion matrix was \hat{Q} for curves 1 and 1', and $2\hat{Q}$ for curves 2 and 2' (see text).

IV. DISCUSSION

In this paper, we introduced a novel technique for inferring the unknown parameters of stochastic nonlinear dynamical systems from time-series data. The key features of our approach are

- a likelihood function written in the form of a path integral over stochastic system trajectories, properly accounting for measurement noise and optimally compensating for dynamical noise; and
- a parameterization of the unknown force field that renders the inference problem essentially linear, despite the strong nonlinearity of the model itself.

Specifically, our analytical derivation produces the correct Jacobian prefactor in the likelihood function, which was missed in earlier works. Meanwhile, the representation of the system nonlinearity as an expansion over a set of basis functions provides stable and robust inference for a broad range of dynamical models. These features enabled us to devise a highly accurate and efficient Bayesian inference algorithm that can reconstruct models of stochastic nonlinear dynamical systems *without* resorting to brute-force numerical optimization.

We illustrated the advantages of our approach by applying it first to the inference of the stochastic nonlinear dynamical system of Lorenz. In the context of parameter estimation with 8 unknown parameters, we showed that the accuracy and efficiency of our algorithm exceed those achieved (under similar conditions) in earlier works. We also demonstrated that our algorithm can deal with the

Lorenz system in the more general setting of model reconstruction, i.e., assuming no knowledge of the functional form of the nonlinear vector field. Although a much larger number of 33 unknown parameters were involved here, our algorithm was still able to achieve a high inference accuracy.

In order to further illustrate the strengths of our algorithm, we applied it next to a system of five coupled nonlinear noisy oscillators. Using a set of polynomial basis functions for the nonlinear field and a full covariance matrix for the dynamical noise, the model comprised 165 unknown parameters, all of which were inferred within an error of 1% from a data set of 10^5 points, taking only a few seconds on a personal computer of average computing power. These demonstrations, we believe, are convincing representation of the capability of our approach, in both accuracy and efficiency, for reconstructing models of stochastic nonlinear dynamical systems.

Furthermore, the efficiency of our algorithm has enabled us recently to identify a stochastic nonlinear model of coupled cardiovascular oscillators using univariate physiological times series data [29] thus opening a new venue for a broad range of important interdisciplinary applications.

Several simplifying assumptions were made here to provide a clear description of the algorithm in its barest form. Although the examples of Section III dealt with noiseless measurements, we have indicated in Section II how measurement noise can be included systematically in our inference algorithm. These examples also required the use of polynomials only, but the approach is in fact completely flexible regarding the type of basis functions used to model the nonlinear force, including time delays. Additionally, the path-integral technique used here to derive the likelihood function allows for a number of straightforward generalizations of our algorithm to the reconstruction of models with colored and multiplicative (or parametric) dynamical noise, and arbitrary (i.e., not necessarily uniform or short) sampling intervals. Finally, although the basic theory of Section II was developed under the implicit assumption that all dynamical variables are available for measurement, we have shown in Section III B that our algorithm is able to reconstruct a complete model from partial measurements of the system trajectory. Since it is often not feasible to measure all degrees of freedom in practice, a generalization of our algorithm to deal with “hidden variables” will be very useful. These extensions will be explored in subsequent publications.

Acknowledgment

This work was supported by the Engineering and Physical Sciences Research Council (UK), NASA CICT-IS-IDU Project (USA), the Russian Foundation for Fundamental Science, and INTAS.

Appendix A
Maximum-likelihood parameter estimation
for a one-dimensional system

Consider a one-dimensional stochastic nonlinear dynamical system

$$\dot{x}(t) = f(x) + \xi(t), \quad (27)$$

where $\xi(t)$ is a zero-mean Gaussian noise process with $\langle \xi(t) \xi(0) \rangle = D \delta(t)$. The mid-point approximation to (27) on the time lattice $\{t_n = t_0 + nh, n = 0, 1, \dots, N\}$ is

$$x_{n+1} = x_n + h f(\tilde{x}_n) + z_n, \quad (28)$$

where we used $x_n \equiv x(t_n)$ and $\tilde{x}_n \equiv \frac{1}{2}(x_{n+1} + x_n)$, and $z_n \equiv \int_{t_n}^{t_{n+1}} \xi(t) dt$ form a sequence of zero-mean Gaussian random variables with $\langle z_n z_{n'} \rangle = h D \delta_{nn'}$.

The probability of realization of a particular random sequence $\{z_n\}$ is

$$\mathcal{P}[\{z_n\}] = \prod_{n=0}^{N-1} \frac{dz_n}{\sqrt{2\pi h D}} \exp\left(-\frac{z_n^2}{2hD}\right). \quad (29)$$

Using the Markovian property of $x(t)$ and the transformation rule $p(\{z_n\}) \prod_n dz_n = p(\{x_n\}) \prod_n dx_n$, along with (28) and (29), we find the probability *density* of the dynamical system trajectory to be

$$p(\{x_n\}) = p_{\text{st}}(x_0) J(\{x_n\}) (2\pi h D)^{-N/2} \times \prod_{n=0}^{N-1} \exp\left\{-\frac{h}{2D} [\dot{x}_n - f(\tilde{x}_n)]^2\right\}, \quad (30)$$

where $\dot{x}_n \equiv (x_{n+1} - x_n)/h$, and the Jacobian of the transformation, to lowest order in h , is

$$J(\{x_n\}) \simeq \prod_{n=0}^{N-1} \left[1 - \frac{h}{2} f'(\tilde{x}_n)\right] \simeq \exp\left[-\frac{h}{2} \sum_{n=0}^{N-1} f'(\tilde{x}_n)\right].$$

Here, prime indicates differentiation with respect to argument. Thus, we obtain for the negative-logarithm of (30) the expression

$$S = -\ln p_{\text{st}}(x_0) + \frac{N}{2} \ln(2\pi h D) + \frac{h}{2} \sum_{n=0}^{N-1} \left\{ f'(\tilde{x}_n) + \frac{1}{D} [\dot{x}_n - f(\tilde{x}_n)]^2 \right\}. \quad (31)$$

Assume now that we observe a time series $\{x_n\}$, and wish to reconstruct a one-dimensional stochastic nonlinear dynamical model for the system that generated the data; i.e., infer the form of the nonlinear function $f(x)$ and estimate the noise intensity D in (27). A fruitful approach to this problem is to model the nonlinearity as a *linear* superposition of a set of nonlinear basis functions:

$$f(x) = \sum_{m=1}^M c_m u_m(x) = \mathbf{c}^T \mathbf{u}(x). \quad (32)$$

The maximum-likelihood (ML) estimates for the unknown model parameters \mathbf{c} and D are then furnished by the global minimum of S . Thus, setting $\partial S/\partial D = 0$ and passing to the limit $h \rightarrow 0$ with $T = Nh$, we find

$$D = \frac{1}{N} \int_{t_0}^{t_0+T} [\dot{x} - \mathbf{c}^T \mathbf{u}(x)]^2 dt. \quad (33)$$

Next, substituting (32) into (31) and rearranging, we obtain $S = \rho - \mathbf{c}^T \mathbf{w} + \frac{1}{2} \mathbf{c}^T \hat{\mathbf{\Sigma}} \mathbf{c}$, where

$$\begin{aligned} \rho &= -\ln p_{\text{st}}(x_0) + \frac{N}{2} \ln(2\pi h D) + \frac{1}{2D} \int_{t_0}^{t_0+T} \dot{x}^2 dt, \\ \mathbf{w} &= \int_{t_0}^{t_0+T} \left[\frac{1}{D} \dot{x} \mathbf{u}(x) - \frac{1}{2} \frac{\partial \mathbf{u}(x)}{\partial x} \right] dt, \\ \hat{\mathbf{\Sigma}} &= \frac{1}{D} \int_{t_0}^{t_0+T} \mathbf{u}(x) \mathbf{u}^T(x) dt. \end{aligned}$$

The condition $\partial S/\partial \mathbf{c} = 0$ now gives

$$\mathbf{c} = \hat{\mathbf{\Sigma}}^{-1} \mathbf{w}. \quad (34)$$

The ML estimates are found by iterating (33) and (34) to convergence.

In Section II, this theory is extended to deal with multi-dimensional system models and to include prior information on model parameters; it is particularly interesting to contrast the results above with our main algorithm given in Section II E.

Appendix B
The generalized least-squares estimator

It is insightful to contrast the algorithm presented in this paper with the generalized least-squares (GLS) estimator. Starting again with the system (1), we neglect measurement noise, adopt the parameterization of (12), and apply the mid-point approximation, obtaining

$$\dot{\mathbf{y}}_n = \hat{\mathbf{U}}_n \mathbf{c} + \boldsymbol{\zeta}_n, \quad n = 0, 1, \dots, N-1, \quad (35)$$

where, as before, we introduced $\dot{\mathbf{y}}_n = (\mathbf{y}_{n+1} - \mathbf{y}_n)/h$ and $\hat{\mathbf{U}}_n = \hat{\mathbf{U}}(\tilde{\mathbf{y}}_n)$ with $\tilde{\mathbf{y}}_n = \frac{1}{2}(\mathbf{y}_{n+1} + \mathbf{y}_n)$. The vectors $\{\boldsymbol{\zeta}_n\}$ satisfy

$$\langle \boldsymbol{\zeta}_n \rangle = \mathbf{0}, \quad \langle \boldsymbol{\zeta}_n \boldsymbol{\zeta}_{n'}^T \rangle = \frac{1}{h} \hat{\mathbf{D}} \delta_{nn'}.$$

We may arrange the N equations contained in (35) into a single partitioned matrix equation as

$$\mathbf{d} = \hat{\mathbf{H}} \boldsymbol{\gamma} + \mathbf{n}, \quad (36)$$

where

$$\hat{\mathbf{H}} = \begin{bmatrix} \hat{\mathbf{U}}_0 & \hat{\mathbf{0}} & \dots & \hat{\mathbf{0}} \\ \hat{\mathbf{0}} & \hat{\mathbf{U}}_1 & \dots & \hat{\mathbf{0}} \\ \vdots & \vdots & \ddots & \vdots \\ \hat{\mathbf{0}} & \hat{\mathbf{0}} & \dots & \hat{\mathbf{U}}_{N-1} \end{bmatrix},$$

$\boldsymbol{\gamma}$ is a column vector comprising N copies of the unknown model coefficient vector \mathbf{c} , and $\mathbf{d} = [\dot{\mathbf{y}}_0 \ \dot{\mathbf{y}}_1 \ \dots \ \dot{\mathbf{y}}_{N-1}]^T$ and $\mathbf{n} = [\zeta_0 \ \zeta_1 \ \dots \ \zeta_{N-1}]^T$ are composite data and noise vectors, respectively, the latter having zero mean and a covariance matrix of the form

$$\langle \mathbf{n} \mathbf{n}^T \rangle = \hat{\boldsymbol{\Lambda}} = \frac{1}{h} \begin{bmatrix} \hat{\mathbf{D}} & \hat{\mathbf{0}} & \dots & \hat{\mathbf{0}} \\ \hat{\mathbf{0}} & \hat{\mathbf{D}} & \dots & \hat{\mathbf{0}} \\ \vdots & \vdots & \ddots & \vdots \\ \hat{\mathbf{0}} & \hat{\mathbf{0}} & \dots & \hat{\mathbf{D}} \end{bmatrix}.$$

Now, the GLS estimator for the vector $\boldsymbol{\gamma}$ in (36) is given by (see, e.g., [28])

$$\boldsymbol{\gamma} = \left(\hat{\mathbf{H}}^T \hat{\boldsymbol{\Lambda}}^{-1} \hat{\mathbf{H}} \right)^{-1} \hat{\mathbf{H}}^T \hat{\boldsymbol{\Lambda}}^{-1} \mathbf{d}. \quad (37)$$

Using the diagonal forms of the matrices $\hat{\mathbf{H}}$ and $\hat{\boldsymbol{\Lambda}}$, we can

extract from (37) the following estimate for our model coefficient vector:

$$\mathbf{c} = \left(\sum_{n=0}^{N-1} \hat{\mathbf{U}}_n^T \hat{\mathbf{D}}^{-1} \hat{\mathbf{U}}_n \right)^{-1} \sum_{n=0}^{N-1} \hat{\mathbf{U}}_n^T \hat{\mathbf{D}}^{-1} \dot{\mathbf{y}}_n. \quad (38)$$

A comparison of (38) with our corresponding result (21) is facilitated by an examination of the definitions (17) and (18), whereupon it is seen that, in the absence of prior information (i.e., $\hat{\boldsymbol{\Sigma}}_{\text{pr}} \rightarrow \hat{\mathbf{0}}$), the only difference between the two estimates is the additional term $\frac{1}{2} \mathbf{v}_n$ in our expression. The importance of this extra term is borne out by the examples given in Section III, where it is observed that the GLS estimator leads consistently to grossly inaccurate parameter estimates, while our algorithm succeeds in achieving arbitrarily high inference accuracy.

-
- [1] K. Visscher, M. J. Schnitzer, and S. M. Block, *Nature* **400**, 184 (1999).
- [2] M. Willemsen, M. P. van Exter, and J. P. Woerdman, *Phys. Rev. Lett.* **84**, 4337 (2000).
- [3] D. J. D. Earn, S. A. Levin, and P. Rohani, *Science* **290**, 1360 (2000).
- [4] J. Christensen-Dalsgaard, *Rev. Mod. Phys.* **74**, 1073 (2002).
- [5] P. Congdon, *Bayesian statistical modelling*, Wiley series in probability and statistics (Wiley, Chichester, 2001).
- [6] G. D'Agostini, *Bayesian reasoning in high-energy physics: principles and applications* (CERN, Geneva, 1999).
- [7] P. E. McSharry and L. A. Smith, *Phys. Rev. Lett.* **83**, 4285 (1999).
- [8] J. P. M. Heald and J. Stark, *Phys. Rev. Lett.* **84**, 2366 (2000).
- [9] R. Meyer and N. Christensen, *Phys. Rev. E* **62**, 3535 (2000).
- [10] R. Meyer and N. Christensen, *Phys. Rev. E* **65**, 016206 (2001).
- [11] J.-M. Fullana and M. Rossi, *Phys. Rev. E* **65**, 031107 (2002).
- [12] S. Siegert, R. Friedrich, and J. Peinke, *Phys. Lett. A* **253**, 275 (1998).
- [13] J. Gradisek, S. Siegert, R. Friedrich, and I. Grabec, *Phys. Rev. E* **62**, 3146 (2000).
- [14] R. Friedrich *et al.*, *Phys. Lett. A* **271**, 217 (2000).
- [15] M. Siefert, A. Kittel, R. Friedrich, and J. Peinke, *Europhys. Lett.* **61**, 466 (2003).
- [16] C. L. Bremer and D. T. Kaplan, *Physica D* **160**, 116 (2001).
- [17] H. Jeffreys, *Theory of Probability*, 3rd ed. (Clarendon Press, Oxford, 1961).
- [18] L. Borland, *Ann. Phys.* **1**, 451 (1992).
- [19] L. Borland, *Z. Phys. B* **88**, 95 (1992).
- [20] L. Borland, *Physica D* **99**, 171 (1996).
- [21] R. Graham, *Z. Phys. B* **26**, 281 (1977).
- [22] E. Gozzi, *Phys. Rev. D* **28**, 1922 (1983).
- [23] M. I. Dykman, *Phys. Rev. A* **42**, 2020 (1990).
- [24] A. K. Rosov, *Nonlinear Filtration of Signals* (Politechnika, St. Petersburg, 2002).
- [25] R. Graham, "Statistical theory of instabilities in stationary non-equilibrium systems with applications to lasers and nonlinear optics," in *Quantum Statistics in Optics and Solid-State Physics*, ed. G. Höhler (Springer-Verlag, Berlin, 1973), Vol. 66, Chap. 1, p. 1.
- [26] J. M. Fulanna, M. Rossi, and S. Zaleski, *Physica D* **103**, 564 (1997).
- [27] R. R. Nigmatulin, *Phys. A* **285**, 547 (2000).
- [28] H. Theil, "Linear algebra and matrix methods in econometrics" in *Handbook of Econometrics*, eds. Z. Griliches and M. Intriligator (North-Holland, New York, 1983), Vol. 1, Chap. 1, p. 5.
- [29] V. N. Smelyanskiy, D. G. Luchinsky, A. Stefanovska *et al.*, "Inference of a nonlinear stochastic model of the cardio-respiratory interaction", to appear in *Phys. Rev. Lett.*